Crystal field analysis of the energy level structure of Cs_2NaAlF_6:Cr^{3+}

Crystal field analysis of the energy level structure of Cs_2NaAlF_6:Cr^{3+}

C Rudowicz[1,6], M G Brik[2,3], N M Avram[4], Y Y Yeung[5] and P Gnutek[1]

[1] Institute of Physics, Szczecin University of Technology, Aleja Piastów 17, 70–310 Szczecin, Poland

[2] Fukui Institute for Fundamental Chemistry, Kyoto University, 34-4 Takano, Nishihiraki-cho, Sakyo-ku, Kyoto 606-8103, Japan

[3] Department of Chemistry, School of Science and Technology, Kwansei Gakuin University, 2-1 Gakuen, Sanda, Hyogo 669-1337, Japan

[4] Department of Physics, West University of Timisoara, Boulevard V. Parvan No. 4, 300223, Timisoara, Romania

[5] Department of Mathematics, Science, Social Sciences and Technology, The Hong Kong Institute of Education, 10 Lo Ping Road, Tai Po, New Territories, Hong Kong SAR, People's Republic of China

E-mail: crudowicz@ps.pl

Abstract

An analysis of the energy level structure of Cr^{3+} ions in Cs_2NaAlF_6 crystal is performed using the exchange charge model (ECM) together with the crystal field analysis/microscopic spin Hamiltonian (CFA/MSH) computer package. Utilizing the crystal structure data, our approach enables modelling of the crystal field parameters (CFPs) and thus the energy level structure for Cr^{3+} ions at the two crystallographically inequivalent sites in Cs_2NaAlF_6. Using the ECM initial adjustment procedure, the CFPs are calculated in the crystallographic axis system centred at the Cr^{3+} ion at each site. Additionally the CFPs are also calculated using the superposition model (SPM). The ECM and SPM predicted CFP values match very well. Consideration of the symmetry aspects for the so-obtained CFP datasets reveals that the latter axis system matches the symmetry-adapted axis system related directly to the six Cr–F bonds well. Using the ECM predicted CFPs as an input for the CFA/MSH package, the complete energy level schemes are calculated for Cr^{3+} ions at the two sites. Comparison of the theoretical results with the experimental spectroscopic data yields satisfactory agreement. Our results confirm that the actual symmetry at both impurity sites I and II in the Cs_2NaAlF_6:Cr^{3+} system is trigonal D_{3d}. The ECM predicted CFPs may be used as the initial (starting) parameters for simulations and fittings of the energy levels for Cr^{3+} ions in structurally similar hosts.

[6] Author to whom any correspondence should be addressed.

1. Introduction

Crystals doped with the Cr^{3+} ion have been receiving considerable attention since 1960, when the first laser was realized with Al_2O_3:Cr^{3+} (Maiman 1960). By now, about 20 other host crystals doped with the Cr^{3+} ion have been shown to lase, thus covering the spectral region between 700 and 1100 nm (Kück 2001). Such wide laser tunability is due to the vibronic interaction between the Cr^{3+} optical electrons and the host lattice ions. The $Cr^{3+}(3d^3)$ ion has a very attractive combination of the spin quartet (e.g., $^4T_{2g}$) and spin doublet (e.g., ^2E) states. Depending on the strength of the crystal (ligand) field (CF), two cases may occur (see, e.g., Henderson and Bartram 2000, Powell 1998). The first excited state is the $^4T_{2g}$ level in a weak CF—this yields the broad emission band; whereas it is the ^2E level in a strong CF— this yields the sharp luminescence lines. Very often several types of impurity centre coexist in the same crystal and it is not always possible to unambiguously distinguish them. Thorough spectroscopic measurements and/or model crystal field calculations are needed in such cases to unravel the nature of the impurity centres.

In this paper, based on the crystal field (CF) theory (see, e.g., Mulak and Gajek 2000, Henderson and Bartram 2000, Powell 1998) we theoretically model the crystal field parameters (CFPs) for the two Cr^{3+} octahedral centres at the crystallographically inequivalent sites (I and II) in Cs_2NaAlF_6 crystal. This enables us to analyse the respective energy level schemes (Sosman *et al* 2000, Torchia *et al* 2002, 2004). Here we do not impose any *a priori* restrictions on the local site symmetry of the impurity sites but first compute the CFPs directly from the crystal structure based on the exchange charge model (ECM) (Malkin 1987). Adoption of the crystallographic axis system centred at the Cr^{3+} ion at each of the two sites I and II may, in general, yield apparent monoclinic- or triclinic-like CFP datasets. However, some non-zero CFPs may be computational artefacts. In order to distinguish such cases, considerations of the symmetry aspects involved in the ECM predicted CFP datasets as well as the resulting energy level splittings have to be carried out. Our analysis reveals that for Cs_2NaAlF_6:Cr^{3+} the crystallographic axis system matches the symmetry-adapted axis system related directly to the six Cr–F bonds well. To ensure the reliability of the ECM results, the CFPs are also calculated using the superposition model (SPM) (Newman and Ng 1989, Mulak and Gajek 2000). The ECM and SPM predicted CFP values match very well. The ECM predicted CFP datasets are used as input for calculations of the complete energy level schemes for Cr^{3+} ions at the two sites in Cs_2NaAlF_6. The computations are carried out using the crystal field analysis/microscopic spin Hamiltonian (CFA/MSH) package (Yeung and Rudowicz 1992, 1993, Chang *et al* 1994, Rudowicz *et al* 2003, Yang *et al* 2003, 2004b, 2004a). Comparison of the theoretical energy levels with the experimental optical spectroscopy data yields satisfactory agreement. Our results enable us to confirm that the actual local site symmetry at the impurity sites I and II in the Cs_2NaAlF_6:Cr^{3+} system is trigonal D_{3d}.

To the best of our knowledge, the calculations presented here constitute the first comprehensive CF analysis for the Cs_2NaAlF_6:Cr^{3+} system. We do not take into account the vibronic interaction and the Jahn–Teller effect since the experimental data on the fine structure of the $^4T_{2g}$ level are scarce for this crystal and our focus is on electronic energy levels. The paper is organized as follows. A brief review of the crystal structure and optical spectroscopy data for the Cs_2NaAlF_6 host is given in section 2. The calculations of the CFPs based on the ECM and the approximate energy level structure as well as those based on the SPM are presented in section 3. The ECM predicted CFPs serve as input for more accurate calculations of the energy level structure using the computer package CFA/MSH presented in section 4. A summary and conclusions are given in section 5.
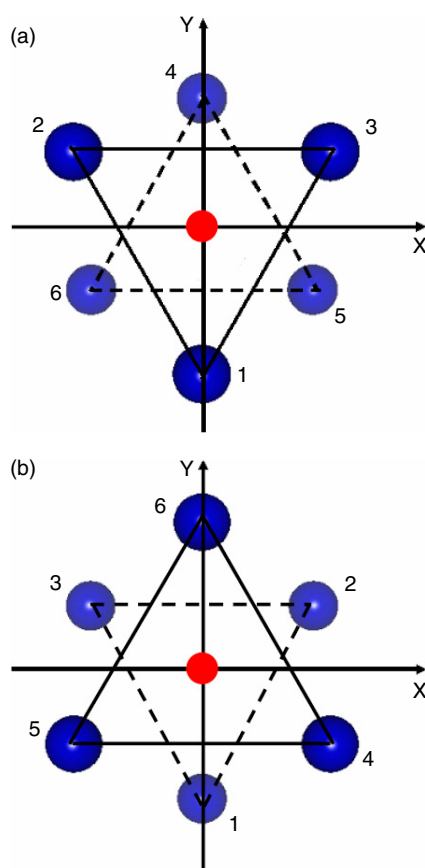
Figure 1. Nearest ligands around the Al^{3+} ion in Cs_2NaAlF_6; the Z axis is directed upward; the chromium ion is at the centre of the fluorine octahedron, whereas the three fluorine ions connected by the solid and dashed lines are located above and below the XY plane, respectively; the positions of atoms are listed in table 1: (a) site I and (b) site II.

(This figure is in colour only in the electronic version)

2. Crystal structure and spectroscopy of Cs_2NaAlF_6:Cr^{3+}

Cs_2NaAlF_6 has a hexagonal perovskite structure with the $R3m$ space group with lattice parameters $a = 0.618\,11$ and $c = 2.9845$ nm (Bordallo *et al* 2001). The unit cell consists of six formula units with 60 ions. There are two crystallographically distinct positions (i.e., site I and site II) and each can be occupied by three Al^{3+} ions. The Cr^{3+} ions substitute for Al^{3+} ions at the octahedral site I or II, each surrounded by six F^- ions (see figures 1(a) and (b), respectively). The Cartesian and angular coordinates of ligands with respect to the crystallographic axes centred at Cr^{3+} ions obtained using the structural data from x-ray and neutron scattering studies (Bordallo *et al* 2001) are listed in table 1. The data in table 1 indicate that the two Al^{3+} sites have an approximate D_{3d} site symmetry since the Al–F_6 complexes are very close to a perfect octahedron with the polar angles θ of the nearest neighbour F^- ligands differing from the perfect case, i.e., 54.74°, by 1.32° and 0.26° for sites I and II, respectively.

Several experimental spectroscopic studies of Cr^{3+}-doped Cs_2NaAlF_6 crystal have recently been reported (Sosman *et al* 2000, Torchia *et al* 2002, 2004, Vrielinck *et al* 2004, da

Table 1. Cartesian (X, Y, Z) (in nm) and angular (R, θ, ϕ) coordinates of F^- ligands in the $[Cr–F_6]^{3-}$ cluster in Cs_2NaAlF_6 referred to the (X, Y, Z) coordinate frame centred at Cr^{3+} (0, 0, 0) obtained using the structural data of Bordallo *et al* (2001).

Ion	X	Y	Z	R (nm)	Θ (deg)	ϕ (deg)
			Site I			
F^-	0	−0.145 601	0.108 039	0.181 31	53.42	270.00
F^-	−0.126 094	0.072 801	0.108 039	0.181 31	53.42	150.00
F^-	0.126 094	0.072 801	0.108 039	0.181 31	53.42	30.00
F^-	0	0.145 601	−0.108 039	0.181 31	126.58	90.00
F^-	0.126 094	−0.072 801	−0.108 039	0.181 31	126.58	330.00
F^-	−0.126 094	−0.072 801	−0.108 039	0.181 31	126.58	210.00
			Site II			
F^-	0	−0.149 063	−0.104 358	0.181 96	125.00	270.00
F^-	0.129 092	0.074 531	−0.104 358	0.181 96	125.00	30.00
F^-	−0.129 092	0.074 531	−0.104 358	0.181 96	125.00	150.00
F^-	0.129 092	−0.074 531	0.104 358	0.181 96	55.00	330.00
F^-	−0.129 092	−0.074 531	0.104 358	0.181 96	55.00	210.00
F^-	0	0.149 063	0.104 358	0.181 96	55.00	90.00

Table 2. Selected experimental energy levels (in cm^{-1}) for Cr^{3+} ions in Cs_2NaAlF_6 (Torchia *et al* 2002; the cross denotes the approximately estimated value) and the energy levels calculated using the initial ECM adjustment procedure (see text). The accuracy of the experimental energies is not provided.

O_h irreps	Experimental values	Calculated (this work)			
		Site I	Averaged	Site II	Averaged
$^4A_{2g}(^4F)$	0	0	0	0	0
$^4T_{2g}(^4F)$	16 129	16 071 16 071 16 243	16 128	16 088 16 151 16 151	16 130
$^4T_{1g}(^4F)$	23 256	22 831 23 464 23 464	23 253	22 705 22 705 22 820	22 743
$^4T_{1g}(^4P)$	26 666†	35 861 35 861 36 999	36 240	35 448 35 754 35 754	35 652

Fonseca *et al* 2000), whereas the spectroscopy of the Cr^{3+} ion in cubic hosts was reviewed by Tanner (2004). The optical absorption spectra of Cs_2NaAlF_6:Cr^{3+} are typical for octahedrally coordinated Cr^{3+} ions. Analysis of the available absorption spectra (Torchia *et al* 2002, 2004) yields the assignment of the experimental energy levels (for the spin-allowed transitions) listed in table 2. However, the $^4A_{2g}(^4F)$–$^4T_{1g}(^4P)$ transition was not observed due to equipment limitations (Sosman *et al* 2000). It was only estimated to be at around 375 nm (26 666 cm^{-1}) by solving the Tanabe–Sugano matrices with the experimentally deduced values (listed below) of the cubic CF parameter Dq and Racah parameters B and C (Sosman *et al* 2000). The emission spectra (Sosman *et al* 2000, Torchia *et al* 2002, 2004) consist of a unique band centred at 12 934 cm^{-1}, which was unambiguously ascribed to the spin-allowed $^4T_{2g}(^4F)$–$^4A_{2g}(^4F)$ transition. More precise analysis of the time-resolved emission spectra (Sosman *et al* 2000)

eliminated two sharp lines at 671 nm (14 903 cm^{-1}) and 701 nm (14 265 cm^{-1}) assigned to the ^{2}E$_g$(^{2}G)–^{4}A$_{2g}$(^{4}F) spin–forbidden transition. Sosman *et al* (2000) have identified two Cr^{3+} sites formed by: (I) three fluorine octahedra connected by their faces and (II) an octahedron linked to two type-I sites through the corners (Babel *et al* 1973, Fargin *et al* 1990). The parameters (Dq, B, C) deduced from the experimental data (Sosman *et al* 2000) are, in cm^{-1}, (1613, 740, 3308) and (1600, 677, 3164) for site I and site II, respectively. Since Dq(II) is slightly smaller than Dq(I), one can expect that the average Cr^{3+}–F$^-$ distance is slightly larger for site II. This expectation is supported by data in table 1, yielding this distance as 0.181 307 nm (site I) and 0.181 963 nm (site II). We note a similar reduction in B and C (due to covalency) as that in Dq (due to CF strength); however, the link between the former quantities and the Cr^{3+}–F$^-$ distance is not as straightforward as in the case of Dq. Additionally, analysis of the electron–phonon coupling of the Cr^{3+} ions in the Cs$_2$NaAlF$_6$ lattice yields the Stokes shift $S = 4.5$ and the effective phonon energy $\hbar\omega = 260$ cm^{-1} (Torchia *et al* 2004).

3. Crystal field theory and the exchange charge model—applications to Cs$_2$NaAlF$_6$:Cr^{3+}

The energy levels of an impurity 3d^N ion in crystals can be described by a Hamiltonian, which includes the free ion terms (see, e.g., Mulak and Gajek 2000, Henderson and Bartram 2000, Powell 1998) and the crystal field Hamiltonian (Malkin 1987):

$$H_{CF} = \sum_{p=2,4} \sum_{k=-p}^{p} B_p^k O_p^k, \tag{1}$$

where the O_p^k are the linear combinations of the tensor operators acting on the angular parts of the wavefunctions, and the B_p^k are the CFPs containing all information about the geometry and nature of an impurity centre. Various types of the spherical tensor operators (STOs) and the tesseral tensor operators (TTOs) used in the electron magnetic resonance (EMR) and optical spectroscopy area have been reviewed by Rudowicz (1987, 1988) and more recently by Rudowicz and Misra (2001). It turns out that the operators actually meant by Malkin (1987) in equation (1) correspond not to the STOs but, in fact, the extended Stevens (ES) operators O_k^q defined by Rudowicz (1985a, 1985b). The ES operators belong to the TTO class and comprise in a unified way also the components O_k^q with negative q. They were introduced as an extension of the *usual* (or *conventional*) Stevens operators, which were originally defined only for $q \geqslant 0$ (Stevens 1952); for details and references, see, Rudowicz (1985a, 1985b, 1987, 1988, 2000a). Although the ES operator notation O_k^q is more widely spread in the literature (Rudowicz 1985a, 1985b, 1987, 1988), below we retain the original Malkin's (1987) notation for the ECM formulation, since the indexed CFPs (i.e., subscript = rank, superscript = component) correspond directly in the two notations. However, the CFPs in equation (1) should not be confused with those in the Wybourne notation B_{kq} (see, e.g., Mulak and Gajek 2000, Rudowicz 1987, 1988), which in some cases are also denoted by the symbol B_p^k (see, e.g., Burdick and Reid 2004).

Originally the ECM was proposed by Malkin (1987) for the rare earth ions, but later it has also been successfully applied to the transition metal ions in different hosts (see, e.g., Jousseaume *et al* 2003, Brik and Avram 2003, 2004, Brik *et al* 2004a, 2004b, 2005, Brik 2005, El-Korashy and Brik 2005). The ECM is an extension of the angular overlap model (AOM) (for a review see, e.g., Schönherr 1997) and it considers both the long- and short-range interactions between an impurity ion and the lattice ions. In the ECM framework, the CFPs can be expressed as a sum of two contributions:

$$B_p^k = B_{p,q}^k + B_{p,S}^k. \tag{2}$$

Table 3. Crystal field parameters (in the extended Stevens notation and in cm^{-1}) calculated in the crystallographic axis system using (i) the initial ECM adjustment procedure and (ii) the superposition model for Cr^{3+} ions at the two sites I and II in Cs_2NaAlF_6; for explanations on the procedures, see text.

Parameter	Point charge contribution	Exchange charge contribution	Total value	Superposition model (cubic approx.)
		Site I		
B_2^0	-6.8	973.4	966.5	—
B_4^{-3}	$16\,403.1$	$61\,874.9$	$78\,278.0$	$77\,556$
B_4^0	-646.1	$-2\,319.7$	$-2\,965.8$	$-2\,908$
		Site II		
B_2^0	-64.4	-199.3	-263.7	—
B_4^{-3}	$-16\,313.9$	$-63\,800.4$	$-80\,114.3$	$-79\,704$
B_4^0	-567.5	$-2\,226.6$	$-2\,794.1$	$-2\,782$

The first term in equation (2) is due to the electrostatic interaction between the 3d electrons of an impurity ion and ligands treated as point charges, whereas the second term, the so-called exchange charge contribution, is proportional to the overlap of the wavefunctions of an impurity ion and ligands, and hence includes all effects of the covalent bond formation and exchange interactions. Taking these effects into account significantly improves the agreement between the calculated energy levels and the experimentally observed ones. The ECM expressions for calculating the contributions to the CFPs in equation (2) derived by Malkin (1987), his equations (2.7) and (2.36), involve for the $3d^N$ ions one dimensionless parameter, G. In the ECM initial adjustment procedure the parameter G is determined by fitting or matching the calculated first absorption band position (or in low symmetry cases the averaged position of the split orbital triplet sublevels) to the observed one. The strong advantage of this ECM procedure is that the so-determined parameter G also enables fitting or matching the higher energy levels with the experimental spectra fairly well.

To increase the accuracy of the calculated $B_{p,q}^k$ contributions arising from various kinds of long-range electrostatic interactions, we need to consider a large cluster around Cr^{3+} ion consisting of 438 ions, namely, 76 Cs^+, 42 Al^{3+}, 50 Na^+ and 270 F^- ions for site I and 88 Cs^+, 42 Al^{3+}, 38 Na^+ and 270 F^- ions for site II. Such clusters involve contributions from ions located at distances up to 1.200 nm (site I) and 1.199 nm (site II). The actual D_{3d} site symmetry around the Cr^{3+} ions doped at the Al^{3+} sites I or II is preserved due to a proper selection of the ions in the large clusters. For the exchange charge contribution $B_{p,S}^k$ only the nearest F^- ligands are taken into account, since the overlap between an impurity ion and ligands from the coordination spheres further than the first one can be safely neglected. Using the ligand positions (table 1) and the Gaussian radial wavefunctions for the Cr^{3+} and F^- ions (Eremin 1989), the initial ECM adjustment procedure yields the CFPs for sites I and II listed in table 3.

A word of caution is necessary here. Our preliminary calculations yielded the CFPs corresponding to symmetry lower than D_{3d} site symmetry expected from table II of Bordallo *et al* (2001) for the two Al^{3+} sites I and II. The judicious choice of the ions is crucial to ensure that the selected cluster preserves the Al^{3+} site symmetry properly. It may not be an easy matter for such a large cluster. In fact, any finite truncation of the crystal lattice for this kind of cluster calculation may potentially lead to an erroneous lowering of the symmetry of the crystal field actually experienced by the central transition ion. Initially we have obtained the

fourth-rank CFPs very close to the trigonal CF case since they were dominated by B_4^{-3} and B_4^0; however, the other non-zero fourth-rank CFPs were smaller than the dominant ones by three to four orders of magnitudes. Such computational artefacts may originate from either inclusion in the lattice summations of some distant ions that do not preserve the site symmetry or some rounding-off errors. After a careful rechecking of the ECM calculations we have eliminated some of the small CFPs due to the former reason as well as significantly reduced the still remaining small CFPs due to the latter reason.

The negligible CFPs, i.e., those with the very small magnitudes, still appearing in the ECM results turn out to be due to unavoidable computational artefacts and are omitted from listing in table 3. Another reason for the eligible non-zero, so 'apparent', low symmetry CFPs is discussed in section 4. Table 3 indicates that taking into account the exchange charge contributions in the CFP calculations is indispensable for obtaining reasonable CFP values and hence for reliable calculated energy levels. The previous studies (Brik and Avram 2003, 2004; Brik *et al* 2004a, 2004b, 2005, 2006a, 2006b; Brik 2005, 2006, El-Korashy and Brik 2005) show that the point charge effects contribute only from 20 to 50% to the total CFP values, whereas the remaining contributions are due to the exchange effects. The final CFPs in table 3 are consistent with the trigonal type I site symmetry (Rudowicz and Qin 2003). Note that by a rotation $\pm 90°/0z$ one can transform B_4^{-3} into $\pm B_4^{+3}$, which is more commonly used in the literature, whereas both parameters are admissible for the continuous rotational symmetry, i.e., trigonal type II, cases (Rudowicz and Qin 2003).

In our calculations the CF Hamiltonian was diagonalized using a separate *Maple* package in the limited subspace of ten wavefunctions belonging to the lowest spin-quartet terms ^4F and ^4P of the Cr^{3+} ion. These terms are chosen because the optical transitions between them are spin-allowed and hence are well identifiable in the spectra. The Racah parameter B, which defines the energy gap between the two terms, was estimated as 740 cm^{-1} (site I) and 667 cm^{-1} (site II) (Sosman *et al* 2000). These values reveal the nephelauxetic effect caused by covalency, i.e., the reduction of the free ion value B_0 to B_c in crystals; taking $B_0(Cr^{3+}) = 918$ cm^{-1} (Powell 1998) yields $\beta = B_c/B_0 = 0.81$ (site I) and $\beta = B_c/B_0 = 0.73$ (site II). A significant nephelauxetic effect for the Cr^{3+} in Cs_2NaAlF_6 indicates a high degree of covalency and serves as a firm justification for including in our calculations both ECM contributions in equation (2). The adjustable parameter G (Malkin 1987) was determined as 4.820 (site I) and 5.007 (site II) by matching the calculated splittings within the ^4F and ^4P terms for Cr^{3+} ions with the experimental ones. The calculated energy levels obtained in this approximate way are listed in table 2 together with the experimental ones.

The absorption bands of the Cr^{3+} ion in Cs_2NaAlF_6 are very broad and were not decomposed into individual bands (Sosman *et al* 2000, Torchia *et al* 2002, 2004). Hence in table 2 we also provide the averaged values of the energies for the group of states arising from the orbital triplets split by the trigonal symmetry CF components. On the other hand, we assume that the barycentre of the group of levels arising from the same triplet corresponds to the energy of the same triplet in O_h symmetry. Table 2 indicates that the energy level scheme calculated for each site agrees fairly well with the experimental spectra (Sosman *et al* 2000, Torchia *et al* 2002, 2004). However, a word of caution should be given about the position of the highest $^4T_{1g}$ (^4P) triplet. Its experimental position was not reported by Sosman *et al* (2000) and Torchia *et al* (2002, 2004), whereas the expected value given by Sosman *et al* (2000) seems to be significantly underestimated. The splitting of the orbital triplets in table 2 into orbital doublets and singlets for Cr^{3+} at both sites I and II correctly reflects the overall trigonal symmetry.

In order to reinforce the validity of our ECM model calculations it is useful to carry out an independent modelling of the CFPs using the superposition model (SPM) (Newman and Ng 1989, Mulak and Gajek 2000). Hence we have also carried out SPM calculations of the CFPs

for Cr^{3+} ions in Cs_2NaAlF_6. Since all nearest F^- neighbour ligands of Cr^{3+} have the same radial distance, whereas the respective polar angles are quite close to the octahedral values, we may adopt the cubic approximation to match the fourth-rank intrinsic SPM parameter $\bar{B}_4$ to the observed energy $E(^4T_2)$ of the $^4T_2$ state. Taking $E(^4T_2)$ as 16 129 and 16 000 cm^{-1} from experimental values (Sosman *et al* 2000), the fitted values of $\bar{B}_4$ are obtained as 9574 and 9709 cm^{-1} for the sites I and II, respectively. Hence, using the SPM formula (Yeung and Newman 1985) the CFP values are obtained within the cubic approximation as listed in the last column of table 3. The results in table 3 indicate that the fourth-rank ECM and SPM predicted CFPs match very well, on average within 1% discrepancy only. Determination of the second-rank CFP within the SPM requires, however, data on other energy levels. Alternatively, the second-rank CFP can be fitted using the conventional trigonal CF parameters v and v' (Yeung and Rudowicz 1992). In fact, if the values of v and v' are available, then we can also determine all the non-cubic CFPs, i.e., $B_2'^0 = B_2^0$ and $B_4'^0$ in the D_{3d} site symmetry, where the primed CFPs are defined by the relation (using the Malkin (1987) index convention): $B_q^k = B_q^k(\text{cubic}) + B_q'^k$.

4. Energy levels calculations for Cs_2NaAlF_6:Cr^{3+} using the CFA/MSH computer package

The computer package CFA (Yeung and Rudowicz 1992, 1993, Chang *et al* 1994) and the improved version CFA/MSH (Rudowicz *et al* 2003, Yang *et al* 2003, 2004b, 2004a) enable us to improve the energy level calculations in section 3, which were based on the initial ECM adjustment procedure. The CFA/MSH package allows obtaining the complete energy level scheme for any $3d^N$ ion in a crystal field of arbitrarily low symmetry within the whole basis of $3d^N$ states, while also taking into account the terms not included by other authors. The energy levels of the impurity ion are obtained by diagonalization of the complete Hamiltonian H within the $3d^N$ basis of states in the intermediate CF coupling scheme. H includes the Coulomb interaction H_{es} (expressed in terms of the Racah parameters B and C or $F^{(2)}$ and $F^{(4)}$), Trees correction $H_{Trees}(\alpha)$, the spin–orbit interaction $H_{SO}(\xi)$, the CF Hamiltonian H_{CF}, the spin–spin interaction H_{SS} and the spin–other orbit interaction H_{SOO} as well as the Zeeman term, which is needed if an external magnetic field is acting upon an impurity ion. For the relevant equations used to calculate the matrix elements of the terms in H we refer to Rudowicz *et al* (2003). Application of the CFA/MSH package to a number of impurity ions (Rudowicz *et al* 2003, Yang *et al* 2003, 2004b, 2004a and references therein) has yielded more accurate results than those based on either approximate calculations within a limited basis of $3d^N$ states or perturbation methods and thus more reliable agreement with the experimental results.

The CFPs listed in table 3 were used as input for the CFA/MSH package to obtain the complete energy level scheme for Cr^{3+}(I) and Cr^{3+}(II) ions in Cs_2NaAlF_6 given in table 4; in this way, a connection between ECM and CFA/MSH is established. Due to the trigonal CF component only the orbital triplets are split, whereas the doublets remain degenerate. From the point of view of the descent in symmetry method it is worthwhile to compare the calculated Cr^{3+} energy levels with those for the ideal octahedral CF labelled by the irreducible representations of the O_h group. The latter energy levels calculated using the experimental sets of Dq, B, and C reported by Sosman *et al* (2000) are also listed in table 4. Comparison of the approximate energy levels (table 2) and the more accurate ones (table 4) indicates their consistency, thus confirming the validity of both approaches.

We note that the sequence of the orbital doublets and singlets arising from the orbital triplets for site I is inverted, in all but one case, as compared with that for site II. This fact is due to the combined effect of the second-rank trigonal CFP B_2^0, which is of opposite signs for

Table 4. The energy levels (in cm^{-1}) calculated using the CFA/MSH package for the Cr^{3+} ions at octahedral sites in Cs_2NaAlF_6: (i) within the cubic CF approximation and (ii) based on the theoretical CFPs obtained from the ECM calculations; the orbital doublet states are indicated by an asterisk.

O_h irrep. repres.	Energy			
	Site I		Site II	
	(i) Cubic CF	(ii) ECM	(i) Cubic CF	(ii) ECM
$^4A_{2g}$	0	0	0	
^2E_g	15 309	15 296	14 467	14 407*
$^2T_{1g}$	15 981	15 915* 16 130	15 066	14 958 15 010*
$^4T_{2g}$	16 130	16 072* 16 244	16 000	16 088 16 151*
$^2T_{2g}$	22 744	22 411 22 906*	21 612	21 515* 21 627
$^4T_{1g}$	23 254	22 831 23 464*	22 671	22 705* 22 820
$^2A_{1g}$	29 014	29 011	28 200	28 290
$^2T_{2g}$	31 311	31 236* 31 469	30 332	30 353 30 421*
$^2T_{1g}$	31 800	31 642 31 851*	30 748	30 775* 30 845
^2E_g	33 603	33 617*	32 451	32 498*
$^4T_{1g}$	36 236	35 862* 37 000	35 484	35 428 35 754*
$^2T_{1g}$	36 816	36 678 36 880*	35 430	35 448* 35 455
$^2T_{2g}$	42 250	42 150* 42 332	40 329	40 233 40 241*
$^2A_{2g}$	43 814	43 785	41 740	41 628
$^2T_{1g}$	47 512	47 391* 47 766	46 356	46 471 46 576*
$^2T_{2g}$	49 392	49 136 49 549*	48 024	48 145* 48 247
^2E_g	52 101	52 128*	49 973	49 929*
$^2T_{1g}$	54 991	54 974* 55 032	53 095	53 154* 53 155
$^2T_{2g}$	70 914	70 536* 71 385	67 948	67 753 67 945*
^2E_g	71 784	71 982*	69 614	69 806*

the two sites, and the non-cubic part of the fourth-rank CFP B_4^{-3}. It is worthwhile to consider the transformations properties of CFPs. A rotation by $\pm 90°$ around the z-axis transforms B_4^{-3} into $\pm B_4^{+3}$, and B_4^{+3} into $\mp B_4^{-3}$, while leaving the parameters B_k^0 invariant. Similarly, a rotation $\pm 180°/0z$ transforms B_4^{-3} into $-B_4^{-3}$, and B_4^{+3} into $-B_4^{+3}$. Since each transformed CFP set is physically equivalent, an arbitrary change of the sign of B_4^{-3} or alternative usage of $\pm B_4^{+3}$

yields the same calculated energy levels. Concerning the exceptional case, i.e., the $^2T_{1g}$ site II data in table 4, in order to verify that no misprint has been made in assigning the asterisk for this case, we have rechecked our calculations. Swapping the asterisk would yield the required consistency, i.e., it might appear at 53 155 (lower number) rather than at 53 154 (upper number). However, the present results are confirmed. It appears that the assignment of the irreps by the CFA program may be computationally doubtful for the near-degenerate cases. We believe that this apparent inconsistency is acceptable since the physical results are still correct as the energy of the doublet and singlet states is nearly the same in this case.

A word of caution should be given here about the meaning of the CFPs calculated in the crystallographic axis system. The minimal set predicted by group theory of the non-zero symbolic CFPs, i.e., the CFPs used to express the CF Hamiltonian, must be referred to an appropriate symmetry-adapted axis system (Rudowicz and Qin 2004). The maximum of 14 non-zero CFPs is required for $3d^N$ ions at triclinic sites, whereas the higher the local site symmetry the smaller the number of such non-zero CFPs. However, in general, the orientation of the crystallographic axes may differ from the symmetry-adapted axes for a given local site symmetry. Then the number of the non-zero theoretical CFPs calculated in the crystallographic axis system may be greater than the number of the non-zero CFPs predicted by group theory in a given symmetry-adapted axis system. The former CFP dataset constitutes an 'apparent' lower symmetry case, which originates due the choice of the axes which do not coincide with the symmetry-adapted axes. In order to consider the inherent low symmetry effects involved in such cases, proper transformations and standardization (Rudowicz and Bramley 1985, Rudowicz 1986, 1991, Rudowicz *et al* 2000) of such CFP datasets must be carried out. To facilitate such computations a novel computer program 3DD based on the idea of diagonalization of the second-rank CFPs like in the case of the zero field splitting (ZFS) parameters (Rudowicz and Qin 2004) has been developed (Rudowicz and Gnutek 2006). Note that incorrect relations between the ZFS parameters in the ES operator notation and the conventional ones for orthorhombic and lower symmetry that have appeared in literature have recently been clarified by Rudowicz (2000a; see therein for references). The program 3DD (Rudowicz and Gnutek 2006) enables finding the principal CFP values and the orientation of the principal axes, whereas the extended computer package CST (Rudowicz 2000b, Rudowicz and Jian 2002) facilitates the corresponding transformations of the fourth-rank CFPs. Illustrative examples of the actual and apparent low symmetry CFP datasets will be considered in forthcoming papers.

In the present case, since the non-zero CFPs in table 3 correlate well with the expectations based on the group theory, the adopted crystallographic axis system turns out to correspond directly to the symmetry-adapted axis system related to the central-ion–ligand bonds. The respective axes have been also indicated in figures 1(a) and (b). Analysis of the nearest ligand coordinates in table 1 shows that the local symmetry for both sites is nearly D_{3d}. The trigonal contributions from the coordination spheres taken into account in our calculations, which lower the approximate cubic site symmetry, are responsible for the partial removal of the degeneracy of the energy levels for both sites I and II.

The reliability of our ECM predicted CFPs in table 3 can be further tested by comparison with data taken from relevant literature. In table 5 we provide a comparative listing of the free ion parameters and the CFPs in the Wybourne notation (see, e.g., Mulak and Gajek 2000, Rudowicz 1987) for Cr^{3+} ions at trigonal sites in various compounds. To facilitate cross-comparison we have converted the respective parameters to the notations most often used in the literature. In order to gauge the 'strength' of the crystal field it is useful to calculate the rotational invariants S_k or equivalently the norms N_k of the CF (ZFS) parameters (for definitions and references, see, Rudowicz and Qin 2003, 2006). Here we provide only the definition of S_k

Table 5. Comparative listing of the free ion parameters: Racah parameters ($F^{(2)}$, F^d), Trees correction (α), and spin–orbit coupling constant (ξ), and the crystal field parameters: conventional cubic CFP (Dq), trigonal CFPs (B_{kq}) in the Wybourne notation (in cm^{-1}), and the respective rotational invariants S_k for Cr^{3+} ions at trigonal sites in various compounds.

	Set	F^b	F^d	α	ξ	Dq	B_{20}	S_2	B_{40}	B_{43}	S_4	Reference
Cs_2NaAlF_6	I	59 416	41 681	—	—	1613	1933	864	−23 726	26 463	14 770	This work
	II	54 831	39 866	—	—	1600	−527	236	−22 353	−27 084	14 783	This work
Cs_2NaGaF_6	1[a]	56 315	40 068	—	—	1535	—	—	—	—	—	da Fonseca *et al* (1999)
	2[a]	58 835	41 517	—	—	1605	—	—	—	—	—	
$LiCaAlF_6$	1[a]	55 244	38 934	—	218	1476	—	—	—	—	—	Avram and Brik (2003)
$KZnF_3$	1[b]	59 570	41 958	—	243	1527	2749	1229	−21 127	−25 657	13 996	Yang (2002)
	2[b]						−3831	1713	−20 292	−26 006	14 002	
	3[b]						−1082	484	−20 040	−26 111	14 005	
$RbCdF_3$	1[a]	62 230	41 454	—	240	1420	—	—	—	—	—	Yang (2000)
$MgAl_2O_4$	1	56 700	40 320	—	250	—	4608	2061	−30 625	−28 415	16 841	Wood *et al* (1968)[e]
Al_2O_3	1[c]	54 589	38 875	—	217.5	1775.4	1045	467	−26 367	−29 708	16 534	Ma *et al* (1999)
	2	53 690	39 312	—	180	—	−1123	502	−22 350	31 538	16 629	Macfarlane (1963)[e]
	3	52 605	37 800	70	—	—	−1123	502	22 400	−31 622	16 672	Fairbank *et al* (1975)*
	4			—	—	—	1425	637	−23 510	−31 166	16 651	McClure (1962)[e]
$LiNbO_3$	1[d]	47 320	36 666	—	—	1532	−3380	1512	−21 335	−25 683	14 041	Jia *et al* (1990)
$ZnAl_2O_4$	1	56 700	40 320	—	250	—	4608	2061	−30 625	−28 415	16 841	Mikenda (1981)[e], Wood *et al* (1968)[e]
	2	56 557	40 370	—	250	—	5321	2380	−32 312	−28 500	17 219	Nie *et al* (1990)[e]
$Y_3Al_5O_{12}$	1	52 724	38 380	132	252	1605	1187	531	−21 574	27 224	14 711	Morrison *et al* (1991)
$Be_3Al_2(SiO_3)_6$	1	55 510	37 296	70	—	—	−5453	2439	−21 123	28 211	15 048	Fairbank *et al* (1975)[e]
	2	58 940	37 296	—	225	—	−7657	3424	−19 690	28 359	14 893	Macfarlane (1970)[e]

[a] Original parameters: B, C.

[b] Original parameters: B, C, ν, ν'; contributions relevant for a given set: #1: (i), #2: (ii), and #3: (i) + (ii), where: (i) K^+-vacancy and (ii) lattice distortion.

[c] Original parameters: B_0, C_0, K_0, K'_0.

[d] Original parameters: B, C, ν, ν'.

[e] As quoted by Morrison (1992).

for the Wybourne notation (see, e.g., Rudowicz and Qin 2006):

$$(S_k)^2 = \frac{1}{2k+1} \sum_q |B_{kq}|^2. \tag{3}$$

The corresponding expressions in the ES notation are provided, for example, by Rudowicz and Qin (2003). Automatic calculation of the quantities S_k for all major tensor operator notations is provided in the package CST (Rudowicz 2000b, Rudowicz and Jian 2002). The quantities S_k are the second-order rank-k rotational invariants and they provide an additional check of compatibility and reliability of experimentally fitted CFPs as well as the consistency of the transformed CFPs expressed in different axis systems by various authors (see, e.g., Rudowicz and Qin 2003, 2004). Table 5 reveals that the values of CFPs and S_k calculated by us fall well within the respective ranges observed and/or calculated by other authors. Hence our literature search enables us additionally to increase the reliability of our results. The closeness of S_4 for sites I and II indicates similar strength of the fourth-rank CF terms for both sites, whereas much smaller B_{20} and thus S_2 for site II than for site I may be explained as follows. Since the second-rank CF terms are identically zero in the perfect octahedral site symmetry, in general, the second-order rank-2 CF invariant S_2 for lower symmetry cases is a measure of the deviation of the site symmetry from the octahedral one (Yeung and Newman 1985, 1986a). The polar angles in table 1 indicate that the Al–F_6 (II) complex is very close to a perfect octahedron. Hence the second-rank CFP B_{20} (II) and thus the invariant S_2 (II) become much smaller in value. This result is also consistent with the experimental finding (Vrielinck *et al* 2004) that the Cr^{3+} ions with the ground state $^4A_2$ have much greater ZFS at site I than at site II. This is due to the fact that the non-cubic second-rank CF term usually makes the dominant contribution to the ground state ZFS for Cr^{3+} ions (Yeung and Newman 1986b).

5. Summary and conclusions

Utilizing the crystal structure data, our approach enables modelling of the crystal field parameters (CFPs) and thus the energy level structure for $3d^N$ ions at arbitrary symmetry sites in crystals. Application to Cr^{3+} ions at the two crystallographically inequivalent sites I and II in Cs_2NaAlF_6 is presented in this paper. Our modelling is based on the exchange charge model (ECM), which has only one adjustable parameter G arising from the overlap effects between wavefunctions of the central ion and ligands. Using the initial ECM adjustment procedure, the CFPs are calculated in the crystallographic axis system centred at the Cr^{3+} ion at each site. This yields large CFPs of trigonal character and a few very small monoclinic- and triclinic-like CFPs datasets, which are identified as computational artefacts. After a careful check of the ECM calculations we have eliminated the very small CFPs. Our results indicate that taking into account the exchange charge contributions in the CFP calculations is indispensable for obtaining reasonable CFP values and thus for reliable modelling of the energy levels schemes for Cr^{3+} ions in Cs_2NaAlF_6. To ensure the reliability of the ECM results, we have also (i) calculated the CFPs using the superposition model (SPM) and (ii) carried out an extensive comparison with data taken from relevant literature for Cr^{3+} ions at trigonal sites in various compounds. The SPM and ECM predicted fourth-rank CFPs show a near perfect agreement, whereas both CFP datasets fall well within the respective ranges observed and/or calculated by other authors.

Computations of the energy level structures of the octahedrally coordinated Cr^{3+} ions in Cs_2NaAlF_6 are carried out using the diagonalization of the CF Hamiltonian within a limited basis of states for the approximate calculations in the initial ECM adjustment procedure, whereas the crystal field analysis/microscopic spin Hamiltonian (CFA/MSH) computer package

is used for the detailed computations within the full basis of states of the $3d^3$ configuration. Comparison of the approximate energy levels and the more accurate ones indicates satisfactory consistency, thus confirming the validity of both approaches. Our calculations for both Cr^{3+} crystallographic sites yield the theoretical energies of the orbital singlet and doublet states arising for the trigonal local site symmetry, which agree well with the experimental data. Provided that an extended range of the experimental energies becomes available, our theoretical energies may be helpful for identification of the transitions in the spectral range above 27 000 cm^{-1}.

Preliminary calculations of the spin Hamiltonian parameters for Cr^{3+} ions at the two sites in Cs_2NaAlF_6 are in progress, utilizing the MSH module within the package CFA/MSH. These considerations are aimed at providing additional verification of the present approach to modelling of the spectroscopic properties. Further applications of the approach presented here to various $3d^N$ ions at low symmetry sites in technologically important crystals will be reported elsewhere (Rudowicz *et al* 2006).

Acknowledgments

References

Avram C N and Brik M G 2003 *J. Lumin.* **102/103** 81
Babel D, Haegele R, Pausewang G and Wall F 1973 *Mater. Res. Bull.* **8** 1371
Bordallo H N, Henning R W, Sosman L P, da Fonseca R J M, Tavares A D Jr, Hanif K M and Strouse G F 2001
    J. Chem. Phys. **115** 4300
Brik M G 2005 *Z. Naturf.* a **60** 437
Brik M G 2006 *J. Phys. Chem. Solids* **67** 738
Brik M G and Avram C N 2003 *J. Lumin.* **102/103** 283
Brik M G and Avram N M 2004 *Z. Naturf.* a **59** 799
Brik M G, Avram C N and Tanaka I 2004 *Phys. Status Solidi* b **241** 2501
Brik M G, Avram N M and Avram C N 2004b *Solid State Commun.* **132** 831
Brik M G, Avram N M, Avram C N and Tanaka I 2005 *Eur. Phys. J. Appl. Phys.* **29** 239
Brik M G, Avram N M and Avram C N 2006a *Spectrochim. Acta* A **63** 759
Brik M G, Avram N M and Avram C N 2006b *Physica* B **371** 43
Burdick G W and Reid M F 2004 *Mol. Phys.* **102** 1141
Chang Y M, Rudowicz C and Yeung Y Y 1994 *Comput. Phys.* **8** 583
da Fonseca R J M, Sosman L P, Tavares A D and Bordallo H N 2000 *J. Fluoresc.* **10** 375
da Fonseca R J M, Tavares A D Jr, Silva P S, Abritta T and Khaidukov N M 1999 *Solid State Commun.* **110** 519
El-Korashy A and Brik M G 2005 *Solid State Commun.* **135** 298
Eremin M V 1989 *Spectroscopy of Crystals* ed A A Kaplyanskii (Leningrad: Nauka) (in Russian)
Fairbank W M, Klauminzer G K and Schawlow A L 1975 *Phys. Rev.* B **11** 60
Fargin E, Lestienne B and Dance J M 1990 *Solid State Commun.* **75** 769
Henderson B and Bartram R H 2000 *Crystal-Field Engineering of Solid-State Laser Materials* (Cambridge: Cambridge
    University Press)
Jia W, Liu H, Knutson R and Yen W M 1990 *Phys. Rev.* B **41** 10906
Jousseaume C, Vivien D, Kahn-Harari A and Malkin B Z 2003 *Opt. Mater.* **24** 143
Kück S 2001 *Appl. Phys.* B **72** 515
Ma D, Zhang H, Liu Y, Chen J and Ma N 1999 *J. Phys. Chem. Solids* **60** 463
Macfarlane R M 1963 *J. Chem. Phys.* **39** 3118

Macfarlane R M 1970 *Phys. Rev.* B **1** 989

Maiman T H 1960 *Nature* **187** 493

Malkin B Z 1987 *Spectroscopy of Solids Containing Rare-Earth Ions* ed A A Kaplyanskii and
   B M Macfarlane (Amsterdam: North-Holland) p 33

McClure D S 1962 *J. Chem. Phys.* **36** 2757

Mikenda W 1981 *J. Lumin.* **26** 85

Morrison C A, Gruber J B and Hills M E 1991 *Chem. Phys.* **154** 437

Morrison C A 1992 *Crystal Fields for Transition-Metal Ions in Laser Host Materials* (Berlin: Springer)

Mulak J and Gajek Z 2000 *The Effective Crystal Field Potential* (Amsterdam: Elsevier)

Newman D J and Ng B 1989 *Rep. Prog. Phys.* **52** 699

Nie W, Michel-Calendini F M, Linares C, Boulen G and Daul C 1990 *J. Lumin.* **46** 177

Powell R C 1998 *Physics of Solid-State Laser Materials* (Berlin: Springer)

Rudowicz C 1985a *J. Phys. C: Solid State Phys.* **18** 1415

Rudowicz C 1985b *J. Phys. C: Solid State Phys.* **18** 3837 (corrigendum)

Rudowicz C 1986 *J. Chem. Phys.* **84** 5045

Rudowicz C 1987 *Magn. Reson. Rev.* **13** 1

Rudowicz C 1988 *Magn. Reson. Rev.* **13** 335 (corrigendum)

Rudowicz C 1991 *Mol. Phys.* **74** 1159

Rudowicz C 2000a *J. Phys.: Condens. Matter* **12** L417

Rudowicz C 2000b *Crystal Field Handbook* ed D J Newman and B Ng (Cambridge: Cambridge University Press)
   p 259

Rudowicz C and Bramley R 1985 *J. Chem. Phys.* **83** 5192

Rudowicz C and Gnutek P 2006 in preparation

Rudowicz C and Jian Q 2002 *Comput. Chem.* **26** 149

Rudowicz C and Misra S K 2001 *Appl. Spectrosc. Rev.* **36** 11

Rudowicz C and Qin J 2003 *Phys. Rev.* B **67** 174420

Rudowicz C and Qin J 2004 *J. Lumin.* **110** 39

Rudowicz C and Qin J 2006 *J. Phys. Conf. Ser.* at press

Rudowicz C, Chua M and Reid M F 2000 *Physica* B **291** 327

Rudowicz C, Yang Z Y, Yeung Y Y and Qin J 2003 *J. Phys. Chem. Solids* **64** 1419

Rudowicz C, Brik M G, Avram N M, Yeung Y Y and Gnutek P 2006 in preparation

Schönherr T 1997 *Top. Curr. Chem.* **191** 87

Sosman L P, Tavares A D Jr, da Fonseca R J M, Abritta T and Khaidukov N M 2000 *Solid State Commun.* **114** 661

Stevens K W H 1952 *Proc. Phys. Soc.* **65** 209

Tanner P A 2004 *Chem. Phys. Lett.* **388** 488

Torchia G A, Schinca D, Khaidukov N M and Tocho J O 2002 *Opt. Mater.* **20** 301

Torchia G A, Martinez-Matos O, Khaidukov N M and Tocho J O 2004 *Solid State Commun.* **130** 159

Vrielinck H, Loncke F, Callens F, Matthys P and Khaidukov N M 2004 *Phys. Rev.* B **70** 144111

Wood D L, Imbusch G F, Macfarlane R M, Kisliuk P and Larkin D M 1968 *J. Chem. Phys.* **48** 5255

Yang Z-Y 2000 *Appl. Magn. Reson.* **18** 455

Yang Z 2002 *J. Magn. Magn. Mater.* **238** 200

Yang Z Y, Rudowicz C and Yeung Y Y 2003 *J. Phys. Chem. Solids* **64** 887

Yang Z Y, Hao Y, Rudowicz C and Yeung Y Y 2004a *J. Phys.: Condens. Matter* **16** 3481

Yang Z Y, Rudowicz C and Yeung Y Y 2004b *Physica* B **348** 151

Yeung Y Y and Newman D J 1985 *J. Chem. Phys.* **82** 3747

Yeung Y Y and Newman D J 1986a *J. Chem. Phys.* **84** 4470

Yeung Y Y and Newman D J 1986b *Phys. Rev.* B **34** 2258

Yeung Y Y and Rudowicz C 1992 *Comput. Chem.* **16** 207

Yeung Y Y and Rudowicz C 1993 *J. Comput. Phys.* **109** 150